ACS OMEGA

Open Access

http://pubs.acs.org/journal/acsodf

Article

Biocompatibility and Antibacterial Properties of NiTiAg Porous Alloys for Bone Implants

Gulsharat A. Baigonakova, Ekaterina S. Marchenko, Ivan I. Gordienko, Victor A. Larikov, Alex A. Volinsky,* and Anna O. Prokopchuk

Cite This: *ACS Omega* 2024, 9, 25638−25645

Read Online

ACCESS | Metrics & More | Article Recommendations | Supporting Information

ABSTRACT: In order to reduce infections, porous NiTi alloys with 62% porosity were obtained by self-propagating high-temperature synthesis with the addition of 0.2 and 0.5 at. % silver nanoparticles. Silver significantly improved the alloys' antibacterial activity without compromising cytocompatibility. An alloy with 0.5 at. % Ag showed the best antibacterial ability against *Staphylococcus epidermidis*. All alloys exhibited good biocompatibility with no cellular toxicity against embryonic fibroblast 3T3 cells. Clinical evaluation of the results after implantation showed a complete absence of purulent-inflammatory complications in all animals. Even distribution of silver nanoparticles in the surface layer of the porous NiTi alloy provides a uniform antibacterial effect.

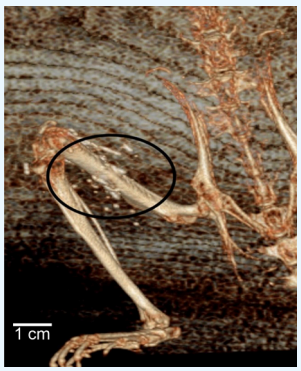

INTRODUCTION

The choice of osteoreplacement material depends on various factors, including specific applications, desired mechanical properties, and biocompatibility. Implants must not interfere with the natural physiology of bone regeneration and must also be able to withstand cyclic loads, ensuring the internal functionality of the skeletal system. It is known that metals, polymers, and ceramics are used as orthopedic biomaterials, but most metals are capable of providing the necessary support due to their mechanical properties.[1,2] Some studies indicate the limited strength of ceramic implants, especially under high loads. Ceramics are more brittle and less flexible than other materials, making them difficult to shape and adapt to a patient's specific anatomy.[3,4] Despite their lightness, flexibility, and biocompatibility, polymer implants have limited strength under high loads and can wear and degrade over time, especially with long-term use.[5] The most common types of metal implants used in bone fractures are titanium alloys, stainless steel, and cobalt−chromium alloys due to their biomechanical and biochemical compatibility.[6−10]

Nickel−titanium (NiTi) porous alloys are the preferred materials for bone implants. Despite porous NiTi alloys being around for many years, their use in medical materials science continues due to fundamental properties, such as mechanical and biological compatibility, increased wear and corrosion resistance in biological environments, and large reversible deformation.[11−13] These alloys are constantly undergoing various modifications in terms of composition, surface modifications, and thermomechanical treatment.[14−16]

Technological parameters of the self-propagating high-temperature synthesis (SHS) determine the implants' porosity and microstructure. The porosity can be adjusted to match the bone tissue and allow its growth into the pores, which promotes bone formation. The protective surface layer spontaneously formed on the surface of porous NiTi alloys during SHS increases its biological compatibility and corrosion resistance.[17] The morphology of the porous NiTi permeable structure is similar to that of bone tissues. Porous NiTi strong superelastic framework retains the support function for bone tissue ingrowth and allows for withstanding alternating physiological loads in the body for a long time.

Despite the obvious advantages of porous NiTi alloys in terms of biochemical and biomechanical compatibility with the body, there is another important area of research dealing with increased antibacterial activity in order to counteract infections at the implant-biological tissue interface.[18−20] Bacteria adhesion to the surface of biomaterials is an important stage of infection development. Infections are accompanied by severe inflammatory processes, leading to bone tissue destruction and implant rejection. Silver is distinguished among noble metals and is bactericidal against a wide range of microorganisms. Silver can be added by different methods,

Received: October 17, 2023
Revised: March 15, 2024
Accepted: March 27, 2024
Published: June 6, 2024

including doping, ion implantation, and coating.[21−24] Nanosized silver has been studied in recent years, including possible mechanisms of silver action in the form of nanoparticles.[22,25−28]

There are mainly studies of monolithic NiTi alloys including NiTiAg. In,[29−31] NiTi composite surface films were doped with 3−10 at. % Ag, which increased the mechanical strength, biocompatibility, and corrosion resistance of implants. However, the alloy's antibacterial properties deteriorated when Ag concentration exceeded 5 at. %. Therefore, doping with lower silver concentrations is of particular interest. The antibacterial activity of the coatings on the NiTi substrates was studied for the 0.2−0.4 wt % Ag range.[32] Coatings containing ≥0.3 wt % Ag showed excellent antibacterial activity. The antibacterial effect was weak at 0.2 wt % Ag concentration. In addition to the concentration, the Ag particle size is also important.

Optimal antibacterial activity, biocompatibility, and corrosion resistance were achieved for the 20−30 nm Ag particle size.[33−35] Ag nanoparticles induce strong antibacterial activity against pathogens in human osteoclasts. It is important that silver nanoparticles in antibacterial concentrations do not have a cytotoxic effect on cells.[36,37] It has been demonstrated that silver nanoparticles provide high antimicrobial efficacy with low cytotoxicity, but cause cellular stress at higher concentrations.[38] For this reason, there must be a balance between antibacterial properties and possible risks to the cells.

There are sporadic studies of the addition of Ag during the sintering of porous NiTi alloys and modifying their surface using Ag. No studies of Ag addition in the preparation of porous NiTi alloys by self-propagating high-temperature synthesis were found. The addition of Ag reduces Young's modulus of the porous NiTi alloys, thereby bringing it closer to Young's modulus of human bones and increasing the maximum deformation of the alloy.[39,40] Thus, this work aims to create a biocompatible antibacterial surface of porous NiTi alloys by adding silver nanoparticles. This research and development will lead to the creation of a class of medical osteoreplacement materials with properties that are superior to existing analogs.[41]

MATERIALS AND METHODS

NiTi alloys with a 62% porosity were obtained by the SHS method in an argon atmosphere from nickel PNK OT-4 powder, titanium PTOM-2 powder, and silver nanopowder with an average particle size of 8 nm with a concentration of 0.2 and 0.5 at. % Ag. For a more uniform distribution of the dopant, silver nanopowder was mixed with nickel powder in amounts close in weight, and then the main part of the nickel and titanium powders was added in portions to the resulting mixture and thoroughly mixed. Samples of the SHS NiTiAg alloy were obtained in a flow reactor with argon to prevent oxidation of the mixture during heating and the synthesized alloy during cooling. The synthesis was initiated by an electric arc after heating the reactor to 420 °C. After the synthesis reaction, the reactor with the resulting porous alloys was cooled by immersion in water at room temperature.

To determine the bactericidal activity, the standard bacteria incubation method in liquid broth was used, followed by seeding on solid media and counting colonies. A daily culture of *Staphylococcus epidermidis* was prepared by transferring 10 μL of a pure culture of microorganisms from agar slant to nutrient broth (400 mL) followed by incubation for 24 h at 25 °C. A day later, 50 μL of the daily culture was placed onto a solid nutrient medium to determine the number of microorganisms in 1 mL of culture. SHS NiTi alloy samples were incubated in a nutrient broth containing a microbial suspension of *Staphylococcus epidermidis* for 72 h at 25 °C. 100 μL aliquot of a whole suspension of microorganisms, at 10^{-6} dilution, was sown on plates with a dense nutrient medium, followed by incubation for 72 h at 25 °C and counting the colony forming units (CFU). In the control, 100 μL of saline was added to the broth. The experiment was carried out three times. Statistical processing was carried out using Microsoft Office Excel 2013, and the significance of differences between the values in the groups was assessed by the Student's *t* test.

To study the cytocompatibility of porous materials, the method of counting stained cells incubated directly on the surface of the implants was used. The method is standard in histology. This approach makes it possible to estimate the number of cells in the top layer of a porous material. Measuring optical density is more suitable for smooth surfaces, since it requires washing off the cell suspension from the surface, which is very difficult for porous materials. NiTi samples were in the form of porous plates 2 × 10 × 10 mm^3 in size with 0.2 at. % and 0.5 at. % concentration of silver nanoparticles. Before the study, the samples were sterilized at 180 °C for 60 min in a dry oven. In the study of cytocompatibility, a standard cell line 3T3 (embryonic fibroblasts) was used. 3T3 cells were cultured in a CO_2 incubator for 72 h under standard conditions at 37 °C, 5% CO_2 and humidified atmosphere. The complete nutrient medium consisted of DMEM/F12 (Paneco, Russia) supplemented with 10% fetal bovine serum (Paneco, Russia), 40 μg/mL gentamicin, and 250 mg/L glutamine. The cells were stained with orange acridine to differentiate live and dead cells. A ZEISS LSM 780 NLO confocal laser scanning microscope was used to count cells in the cytocompatibility experiment. The experiment on each sample was carried out three times by counting cells in 200 × 200 $μm^2$ areas.

The cells were visualized by using a TermoFisher Axia (USA) scanning electron microscope. Samples were washed with a phosphate-buffered saline (PBS) solution and fixed with 2.5% glutaraldehyde for 1 h. The sample was washed three times with PBS for 15 min, fixed in 1% osmium tetroxide (SIGMA) for 1 h, and washed again three times with PBS for 15 min. Then, it was dehydrated by successive changes in the volume concentration of ethanol (30, 50, 70, 90, and 100%) for 15 min in each solution. The samples were dried.

The experimental study was carried out in the vivarium of the Ural State Medical University (Stukova N.A., head of the vivarium) in accordance with the "European Convention for the Protection of Vertebrate Animals used for Experimental and Other Scientific Purposes" (Strasbourg, France, 1986). Experiments aimed at studying the NiTi alloys, approved by the local ethics committee of the Ural State Medical University, extract from protocol No. 6 dated 06/17/2022. All animals were kept following sanitary requirements No. 1045−73 of 04/06/1973. The experiment was carried out on 9 sexually mature female white laboratory rats, weighing 400−600 g. Rats were divided into 3 groups of 3 individuals, and all animals were implanted with NiTi with silver additives in the form of porous granules. The granules were obtained by the mechanical grinding of porous ingots. The first group was the

https://doi.org/10.1021/acsomega.3c08163
ACS Omega 2024, 9, 25638−25645

control group, the second with 0.2 at. % silver, and the third group with 0.5 at. % silver.

RESULTS AND DISCUSSION

The phase and elemental composition, along with mechanical properties of NiTiAg alloys with a silver concentration of 0, 0.2, and 0.5 at. % were studied in earlier work.[42] X-ray diffraction (XRD) and energy dispersive spectroscopy (EDS) data showed limited silver solubility up to 0.1 at. % in the TiNi(B2) intermetallic phase. It was also shown that an increase in the silver concentration leads to the crystallization of silver nanoparticles mainly in the zones of peritectic crystallization of the Ti_2Ni intermetallic compound, increasing the porous NiTi alloy plasticity from 7 to 27% while maintaining 70 ± 4 MPa compressive strength. Studies of the structure and mechanical properties of porous NiTi alloyed with silver have shown positive prerequisites for these studies. Therefore, in this work, the biocompatibility and antibacterial action of porous NiTiAg alloys were studied, which are important characteristics for the use of these alloys for medical purposes.

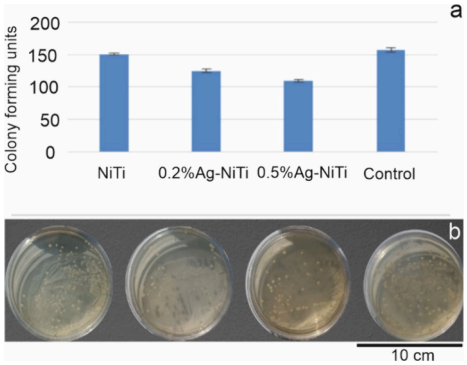

Figure 1. Antibacterial activity against *Staphylococcus epidermidis*: (a) colony forming units; (b) examples of inoculations on solid agar from the left to right: NiTi, NiTi + 0.2 at. % Ag, NiTi + 0.5 at. % Ag, control without a sample. Error bars represent the standard deviation in (a).

Antibacterial Properties and Cytocompatibility Study. *Staphylococcus epidermidis* was chosen as the bacteria in the antimicrobial experiment. The indicators of antibacterial activity of samples with different silver contents are shown in Figure 1. Bacteria suspension without a sample was used as a control. Since silver is a biocidal additive, it is advisable to study the antibacterial properties of NiTi alloys with silver compared to NiTi without silver (Figure 1, NiTi) and a suspension of bacteria without a sample (Figure 1, Control) as a control for bacteria experiments in order to demonstrate that the active substance is Ag. The antibacterial effects of the samples against *Staphylococcus epidermidis* gradually increased with Ag concentration. The significance of the differences between the experiment and the control was confirmed by Student's test $p < 0.05$, while the sample not containing Ag and the control did not differ significantly. Thus, it can be concluded that the NiTiAg alloys have bioactive properties due to the Ag addition. An alloy with 0.5 at. % Ag concentration showed the best antibacterial ability against *Staphylococcus epidermidis* in Figure 1a.

A cytocompatibility study was performed using porous NiTi samples with different silver content and visualization of cells using a scanning electron microscope. Different densities of cell cultures are observed on the surface of the studied alloys, as shown in Figure 2. It should be noted that the addition of 0.5 at. % Ag leads to a decrease in the number of cells on the surface of the porous NiTi alloy, while more cells were found on the alloy with 0.2 at. % Ag.

The obtained data are in good agreement with the results of other authors. Current literature reports the antibacterial and antiviral effects of silver nanoparticles. Silver has bactericidal activity at concentrations up to 35 ppb without toxic effects on mammalian cells. Silver concentrations >0.01 mmol/L have been reported to be cytotoxic.[43] In another study, there was no evidence of silver toxicity in a fibroblast cell line until silver concentration reached 1200 ppb.[44] In vivo testing has shown that toxic side effects such as argyrosis, leukopenia, and liver and kidney damage occur when silver concentration in blood exceeded 300 ppb.[45] All of these critical concentrations causing toxicity are higher than the Ag concentration used in this work. It was found that the silver addition up to 3 at. % leads to improved NiTi tribological properties, cytocompatibility, and biocompatibility.[46,47] Toxicological studies have shown the safety of small concentrations of silver nanoparticles in humans and the environment. NiTiAg alloy with a 0.5 at. % silver concentration has improved properties, including cytocompatibility and antibacterial ability, along with increased yield strength and tensile strength.[48−53] Ag addition to NiTi alloys shows obvious inhibition of bacteria growth.

According to the experimental data, the average number of living cells differed significantly in the samples and the control, as shown in Figure 3. Here, the average number of cells was counted in three 200 × 200 μm^2 inspection regions for each sample. The number of dead cells is the same in all groups. Also, in all three groups, there are significantly more living cells than dead and apoptotic cells ($p = 0.05$).

Thus, all three alloys are cytocompatible. The Ag content increases the number of cells in apoptosis, but the number of dead cells in all samples is equally low, which may indicate a moderate cytotoxic effect. However, analysis of the top layer and cell morphology showed that the surface of the alloy was

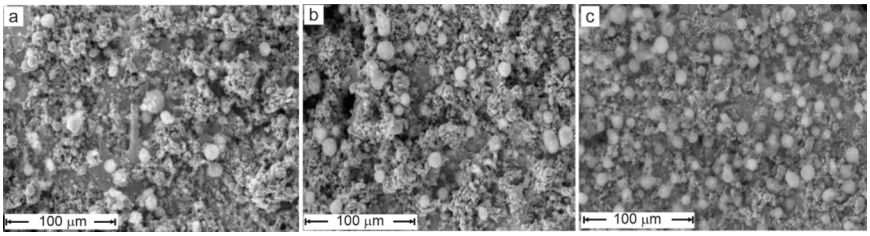

Figure 2. Scanning electron microscopy images of the porous alloys' surface after cells cultivation: (a) NiTi; (b) NiTi + 0.2 at. % Ag; (c) NiTi + 0.5 at. % Ag.

https://doi.org/10.1021/acsomega.3c08163
ACS Omega 2024, 9, 25638−25645

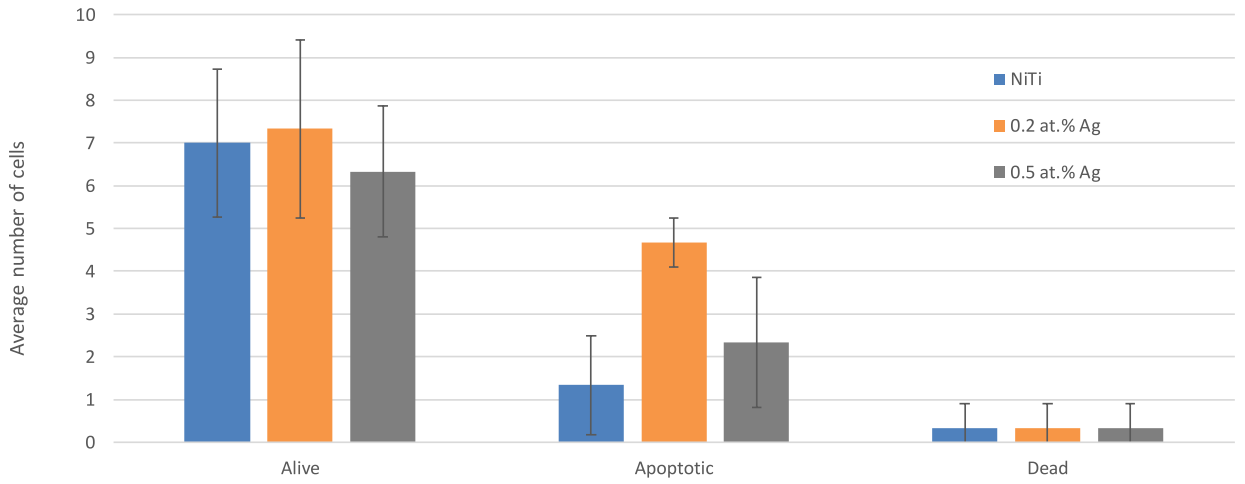

Figure 3. Quantitative analysis of cell viability on the porous NiTi alloys' surfaces. Error bars represent the standard deviation.

Figure 4. Macro-operation of the femur of a laboratory rat implanted with NiTi with 0.5 at. % Ag in the distal part 75 days after implantation.

covered with a dense monolayer. The porous material allows the cells to develop an extracellular matrix, in contrast to the flat surface, which mimics the conditions of growth in a cellular environment in body tissues. Cells had an irregular shape, typical for the 3T3 cell line. In the analysis of cytocompatibility, all alloys retained good biocompatibility and did not show cellular toxicity against embryonic fibroblast 3T3 cells.

In Vivo Tests. Surgical treatment of laboratory rats was carried out under sterile conditions and general anesthesia. Anesthesia was administered by an intramuscular injection of Zoletil 100 at 10 mg/kg of body weight. After preparation of the surgical table, hair removal, and treatment with antiseptic solutions, operative access was made by cutting the skin to 2

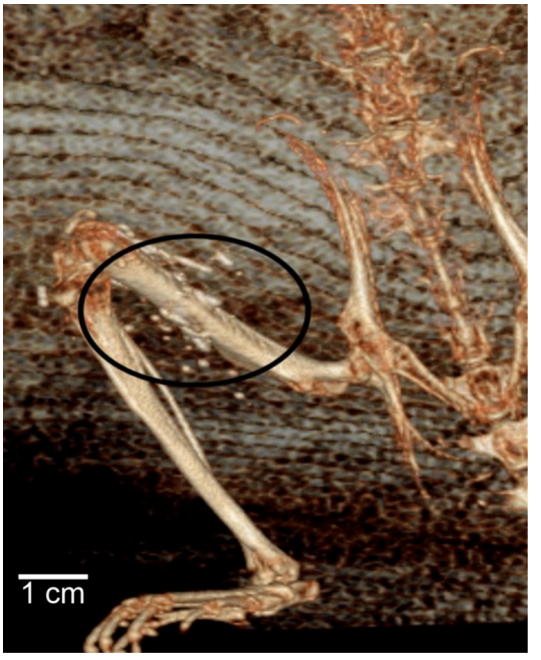

Figure 6. 3D CT image of a laboratory rat. The site of implantation in the bone and surrounding soft tissues is highlighted. 75 days after implantation.

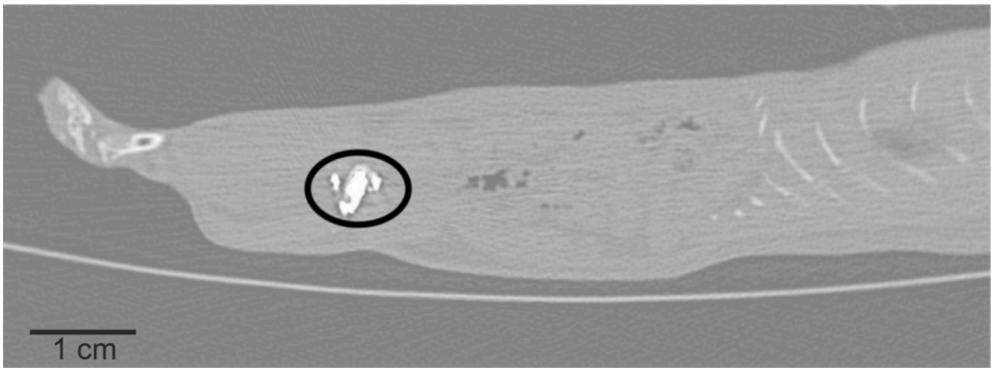

Figure 5. Sagittal CT scan of a laboratory rat. Selected material was installed in the medullary canal of the femur. 75 days from implantation.

https://doi.org/10.1021/acsomega.3c08163
ACS Omega 2024, 9, 25638−25645

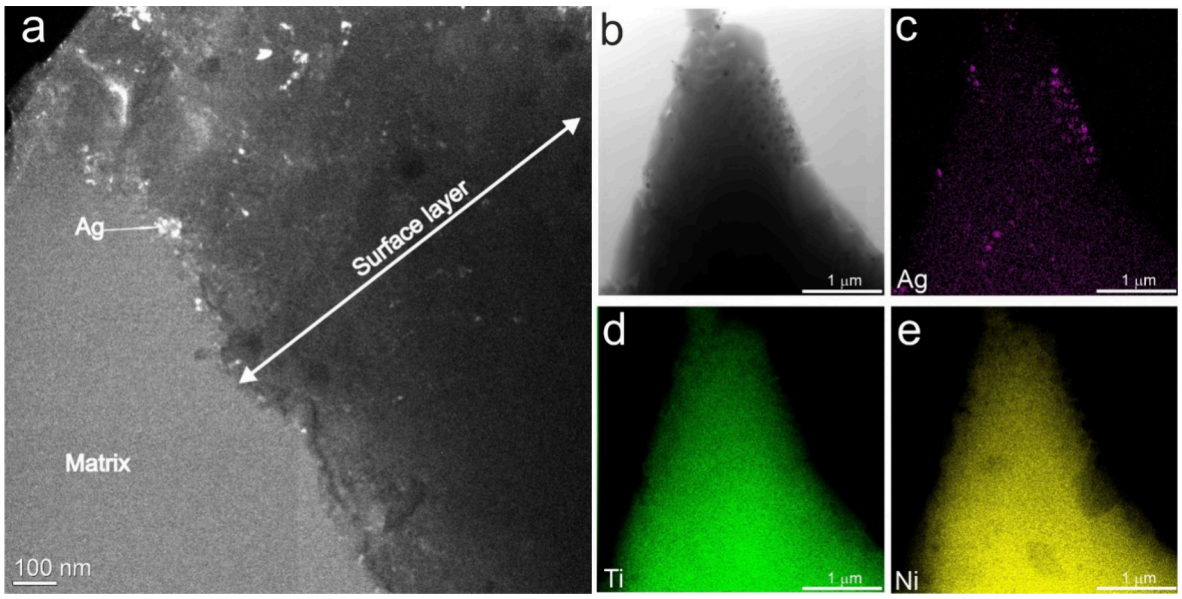

Figure 7. Distribution of Ag in the NiTi + 0.5 at. % Ag sample: (a) TEM cross-section; (b−e) EDS elemental mapping.

cm along the outer surface of the right thigh. The femur was isolated, and using an engraver with a sterile club-shaped tip, a refinement hole was made in the proximal meta-diaphyseal region of the femur with 0.3 × 0.3 cm^2 dimensions. In the process of accessing the femur, the sharp way with a scalpel was used to dissect dense tissues (skin, fascia, periosteum), and the blunt way with a mosquito clamp to separate loose tissues (subcutaneous fat and muscles), since the muscles dissected in the hip area will entail a sharp decrease in the rat's activity in the postoperative period, affecting the purity of the experiment. At this stage, a model of the cavity formation of a tubular bone was obtained. Then, using a Volkmann spoon, a fine powder of NiTi was implanted into the formed bone cavity depending on the group. The material was tightly packed into the bone; however, part of the material got into the soft tissues near the bone, which is acceptable. The operation was completed with layer-by-layer sutures of the wound and treatment of the main access area with brilliant green. The postoperative period was uneventful, and anesthesia was performed with Flexoprofen 2.5% at 2.5 mg/kg of body weight. When alloys with a silver concentration of 0.5 at. % were used, the healing process proceeded faster. On the 75th day, all animals were withdrawn from the experiment by an overdose of the anesthetic drug, followed by the sampling of the femurs for further histological examination of the bone-implant interface and electron microscopy in Figure 4. 75 days from the bone tissue damage is double the time for consolidation and the appearance of the callus of the femur (30−35 days average consolidation time). This time period was chosen due to the special type of modeling of the pathological process. This is not just a bone fracture but the formation of a pathological bone cavity thinning of the cortical layers from the inside. It was also taken into account that the bone tissue damage area here is greater than with a normal fracture, and there is also interaction with foreign material.

When conducting a clinical evaluation of the results, there was a complete absence of purulent-inflammatory complications in all animals at all stages of the experiment. Before the animals were removed, there were no signs of inflammation in the area of material implantation during a clinical examination; palpation was painless; the local temperature was not elevated; and the movement of animals in the cage was not difficult. On the 75th day, the animals underwent computed tomography (CT), which showed a good filling of the bone defect, and the absence of a dystrophic effect in the area of contact of the bone and soft tissues with the material, as shown in Figures 5 and 6.

Spongy tissue formation requires from 4 to 12 weeks, while the presence of postoperative infectious complications does not allow the newly formed bone tissue to fill the formed spaces in a timely manner, and increases the rehabilitation time.[54−58] CT control of all groups of animals showed that the osseointegration of alloys with 0.5 at. % Ag begins immediately after implantation and ends 2 weeks earlier than in the control group. To confirm the rate of material osseointegration, a comparative assessment of the Hounsfield scale was used, which determines the material density from the gray scale of each pixel in the image. The intact cortical bone tissue density of a laboratory animal is 250−350 HU. The bone tissue density at the bone-implant interface was assessed along the axial projection perimeter during CT characterization. The alloy density with 0.5 at. % Ag was higher (210−270 HU) compared with the control group (110−170 HU), which may indicate a lower osseointegration degree and rate.

To understand the mechanisms of antibacterial activity, improved cytocompatibility, and survival, transmission electron microscopy (TEM) studies of the porous alloys with 0.5 at. % Ag were carried out, as shown in Figure 7.

Based on the TEM results of NiTi samples with 0.5 at. % Ag in the cross-section geometry, silver was found in the form of nanoparticles up to 10 nm in size evenly distributed in the Ti_4Ni_2O surface layer in Figure 7. The presence of silver nanoparticles provided the antibacterial effect due to the standard mechanism described in several references[22−28] demonstrating the release of pure silver ions from the surface into the adjacent liquids.

On the one hand, uniformly distributed nanostructured silver ensures a uniform antibacterial effect due to the low solubility of silver in NiTi. Silver dissolves in the TiNi(B2) phase of the porous alloy up to 0.1 at. %, while other authors found that the solubility of silver in the cast alloy does not

https://doi.org/10.1021/acsomega.3c08163
ACS Omega 2024, 9, 25638−25645

exceed 0.26 at. %.[59−61] On the other hand, the Ti_4Ni_2O surface layer on porous NiTi alloys obtained by the SHS is very active, as it adsorbs light impurities as a getter.[62,63] Therefore, as pointed out in several references, the mechanism of silver action on a microbial cell is achieved by the absorption of silver ions by the microbial cell membrane, and as a result, the cell remains alive, but its division is disturbed and a bacteriostatic effect is achieved.

CONCLUSIONS

The biocompatibility and antibacterial effects of the surface of porous NiTi alloys with silver nanoparticles have been experimentally confirmed under in vitro and in vivo conditions. It has been established that with an increase in the concentration of silver nanoparticles to 0.5 at. % the antibacterial activity increases. The porous NiTi alloy with 0.5 at. % silver turned out to be the most antibacterial and cytocompatible. Clinical experimental evaluation on laboratory rats of all groups of animals showed that the osseointegration of alloys with 0.5 at. % Ag begins immediately after implantation and ends 2 weeks earlier than in other groups. The observed positive effect is related to the uniform crystallization of silver nanoparticles in the Ti_4Ni_2O surface layer.

ASSOCIATED CONTENT

Data Availability Statement

The data used to plot Figures 1a and 3 were submitted to the journal with the paper. The rest of the data are presented in the body of the paper as images.

Supporting Information

The Supporting Information is available free of charge at https://pubs.acs.org/doi/10.1021/acsomega.3c08163.

Cell experiments and a table showing the average number of cells (PDF)

AUTHOR INFORMATION

Corresponding Author

Alex A. Volinsky − *Laboratory of Superelastic Biointerfaces, National Research Tomsk State University, 634045 Tomsk, Russia; Department of Mechanical Engineering, University of South Florida, Tampa, Florida 33620, United States;* orcid.org/0000-0002-8520-6248; Email: volinsky@usf.edu

Authors

Gulsharat A. Baigonakova − *Laboratory of Superelastic Biointerfaces, National Research Tomsk State University, 634045 Tomsk, Russia*

Ekaterina S. Marchenko − *Laboratory of Superelastic Biointerfaces, National Research Tomsk State University, 634045 Tomsk, Russia*

Ivan I. Gordienko − *Department of Pediatric Surgery, Ural State Medical University, 620014 Yekaterinburg, Russia*

Victor A. Larikov − *Laboratory of Superelastic Biointerfaces, National Research Tomsk State University, 634045 Tomsk, Russia*

Anna O. Prokopchuk − *Laboratory of Superelastic Biointerfaces, National Research Tomsk State University, 634045 Tomsk, Russia*

Complete contact information is available at: https://pubs.acs.org/10.1021/acsomega.3c08163

Author Contributions

G.A.B.: Conceptualization, Visualization, Writing—review, and editing. E.S.M.: Writing−review and editing, Supervision, Resources, Project administration, Funding acquisition. I.I.G.: Methodology, Resources, Investigation, Formal analysis. V.A.L.: Conceptualization, Investigation, Writing—review and editing. A.A.V.: Writing—review, and editing, Project administration. A.O.P.: Methodology, Resources, Data curation.

Notes

The authors declare no competing financial interest.

ACKNOWLEDGMENTS

The study was supported by the Russian Science Foundation, grant 22-72-10037, https://rscf.ru/project/22-72-10037/

REFERENCES

(1) Ratner, B.D.; Hoffman, A.S.; Schoen, F.J.; Lemons, J.E. *Biomaterials science: An introduction to materials in medicine*; Elsevier, 2004.

(2) Kim, T.; See, C.; Li, X.; Zhu, D. Orthopedic implants and devices for bone fractures and defects: past, present and perspective. *Eng. Regen.* **2022**, *1*, 6−18.

(3) Fernandez, G.; Laetitia, K.; Ysia, I.; Quentin, W.; Anne-Marie, M.; Benkirane-Jessel, N.; Bornert, F.; Offner, D. Bone substitutes: a review of their characteristics, clinical use, and perspectives for large bone defects management. *J. Tissue Eng.* **2018**, *9*, No. 2041731418776819, DOI: 10.1177/2041731418776819.

(4) Marti, A. Inert bioceramics (Al2O3, ZrO2) for medical application. *Injury* **2000**, *31*, 33−36.

(5) Deshmukh, R.; Kulkarni, S. A review on biomaterials in orthopedic bone plate application. *Int. J. Curr. Eng. Technol.* **2015**, *5*, 2587−2591.

(6) Disegi, J.; Eschbach, L. Stainless steel in bone surgery. *Injury* **2000**, *31*, 2−6.

(7) Bekmurzayeva, A.; Duncanson, W.; Azevedo, H.; Kanayeva, D. Surface modification of stainless steel for biomedical appli-cations: revisiting a century-old material. *Mater. Sci. Engin C* **2018**, *93*, 1073−1089.

(8) Wojnar, L.; Dabrowski, J.; Oksiuta, Z. Porosity structure andmechanical properties of vitalium-type alloy for implants. *Mater. Charact.* **2001**, *46*, 221−225.

(9) Hayes, J.; Richards, R. The use of titanium and stainless steel in fracture fixation. *Expert review of medical devices* **2010**, *7*, 843−853.

(10) Eliaz, N. Corrosion of metallic biomaterials: A review. *Materials* **2019**, *12*, 407.

(11) Gunter, V.; Yasenchuk, Y.; Gunther, S.; Ekaterina, M.; Yuzhakov, M. Biocompatibility of porous SHS-TiNi. *Mater. Sci. Forum* **2019**, *970*, 320−327.

(12) Topolnitskiy, E.; Chekalkin, T.; Marchenko, E.; Yasenchuk, Yu.; Kang, S.-B.; Kang, J.-H.; Obrosov, A. Evaluation of clinical performance of tini-based implants used in chest wall repair after resection for malignant tumors. *Journal of Functional Biomaterials* **2021**, *12*, 60.

(13) Sevilla, P.; Aparicio, C.; Planell, J.; Gil, F. Comparison of the mechanical properties between tantalum and nickel-titanium foams implant materials for bone ingrowth applications. *J. Alloys Compd.* **2007**, *439*, 67−73.

(14) Hornbogen, E. Microstructure and thermo mechanical properties of NiTi shape memory alloys. *Mater. Sci. Forum* **2004**, *455−456*, 335−341.

(15) Shen, J.; Lu, N.; Chen, C. Mechanical and elastocaloric effect of aged Ni-rich TiNi shape memory alloy under load-controlled deformation. *Materials Science and Engineering* **2020**, *788*, No. 139554.

(16) Marchenko, E.; Luchsheva, V.; Baigonakova, G.; Bakibaev, A.; Vorozhtsov, A. Functionalization of the surface of porous nickel-titanium alloy with macrocyclic compounds. *Materials* **2023**, *16*, 66.

(17) Marchenko, E.; Baigonakova, G.; Yasenchuk, Y.; Chekalkin, T.; Volinsky, A. Structure, biocompatibility and corrosion resistance of the ceramic-metal surface of porous nitinol. *Ceram. Int.* **2022**, *48*, 33514−33523.
(18) Oh, K.; Joo, U.; Park, G.; Hwang, C.; Kim, K. Effect of silver addition on the properties of nickel-titanium alloys for dental application. *J. Biomed. Mater. Res.* **2006**, *76*, 306−314.
(19) Zhao, L.; Chu, P.; Zhang, Y.; Wu, Z. Antibacterial coatings on titanium implants. *J. Biomed. Mater. Res.* **2009**, *91*, 470−480.
(20) Chouirfa, H.; Bouloussa, H.; Migonney, V.; Falentin-Daudre, C. Review of titanium surface modification techniques and coatings for antibacterial applications. *Acta Biomaterialia* **2019**, *83*, 37−54.
(21) Ferraris, S.; Spriano, S. Antibacterial titanium surfaces for medical implants. *Materials Science and Engineering: C* **2016**, *61*, 965−978.
(22) Schmidt-Braekling, T.; Streitbuerger, A.; Gosheger, G.; Boettner, F.; Nottrott, M.; Ahrens, H.; Dieckmann, R.; Guder, W.; Andreou, D.; Hauschild, G.; Moellenbeck, B.; Waldstein, W.; Hardes, J. Silver-coated megaprostheses: review of the literature. *European Journal of Orthopaedic Surgery and Traumatology* **2017**, *27*, 483−489.
(23) Liu, X.; Gan, K.; Liu, H.; Song, X.; Chen, T.; Liu, C. Antibacterial properties of nano-silver coated PEEK prepared through magnetron sputtering. *Dent. Mater.* **2017**, *33*, 348−360.
(24) Fu, S.; Zhang, Y.; Qin, G.; Zhang, E. Antibacterial effect of TiAg alloy motivated by Ag-containing phases. *Materials Science and Engineering: C* **2021**, *128*, No. 112266.
(25) Kim, J.; Kuk, E.; Yu, K.; Kim, J.; Park, S.; Lee, H.; Kim, S.; Park, Y.; Park, Y.; Hwang, C.; Kim, Y.; Lee, Y.; Jeong, D.; Cho, M. Antimicrobial effects of silver nanoparticles, Nanomedicine: Nanotechnology. *Biol. Med.* **2007**, *3*, 95−101.
(26) Aurore, V.; Caldana, F.; Blanchard, M.; Kharoubi Hess, S.; Lannes, N.; Mantel, P.-Y.; Filgueira, L.; Walch, M. Silver-nanoparticles increase bactericidal activity and radical oxygen responses against bacterial pathogens in human osteoclasts. *Nanomedicine* **2018**, *14*, 601−607.
(27) Praba, V.; Kathirvel, M.; Vallayyachari, K.; Surendar, K.; Muthuraj, M.; Jesuraj, P.; Govindarajan, S.; Raman, K. Bactericidal effect of silver nanoparticles against mycobacterium tuberculosis. *Journal of Bionanoscience* **2013**, *7*, 282−287.
(28) Van Dong, P.; Ha, C. H.; Binh, L. T.; Kasbohm, J. Chemical synthesis and antibacterial activity of novel-shaped silver nanoparticles. *Int. Nano Lett.* **2012**, *2*, 9 DOI: 10.1186/2228-5326-2-9.
(29) Zamponi, C.; Wuttig, M.; Quandt, E. Ni−Ti−Ag shape memory thin films. *Scripta Materialia* **2007**, *56*, 1075−1077.
(30) Quandt, E.; Zamponi, C. Superelastic NiTi thin films for medical applications. *Adv. Sci. Technol.* **2008**, *59*, 190−197.
(31) Thangavel, E.; Dhandapani, V.; Dharmalingam, K.; Marimuthu, M.; Veerapandian, M.; Arumugam, M.; Kim, S.; Kim, B.; Ramasundaram, S.; Kim, D. RF magnetron sputtering mediated NiTi/Ag coating on Ti-alloy substrate with enhanced biocompatibility and durability. *Materials Science and Engineering: C* **2019**, *99*, 304−314.
(32) Liu, Z.; Xiao, K.; Hou, Z.; Yan, F.; Chen, Y.; Cai, L. Multifunctional coating with both thermal insulation and antibacterial properties applied to nickel-titanium alloy. *Int. J. Nanomed.* **2020**, *15*, 7215−7234.
(33) Sharma, A.; Singh, R.; Tiwari, A.; Sharma, A. Enhancement of physical and mechanical characteristics of NiTi composite containing Ag and TiC. *Journal of Materials Engineering and Performance* **2022**, *31*, 2934−2945.
(34) Chen, M.; Yang, L.; Zhang, L.; Han, Y.; Lu, Z.; Qin, G.; Zhang, E. Effect of nano/micro-Ag compound particles on the bio-corrosion, antibacterial properties and cell biocompatibility of Ti-Ag alloys. *Materials Science and Engineering: C* **2017**, *75*, 906−917.
(35) Martinez-Gutierrez, F.; Olive, P.; Banuelos, A.; Orrantia, E.; Nino, N.; Sanchez, E.; Ruiz, F.; Bach, H.; Av-Gay, Y. Synthesis, characterization, and evaluation of antimicrobial and cytotoxic effect of silver and titanium nanoparticles, Nanomedicine: Nanotechnology. *Biol. Med.* **2010**, *6*, 681−688.
(36) Albers, C.; Hofstetter, W.; Siebenrock, K.; Landmann, R.; Klenke, F. In vitro cytotoxicity of silver nanoparticles on osteoblasts and osteoclasts at antibacterial concentrations. *Nanotoxicology* **2013**, *7*, 30−36.
(37) Aurore, V.; Caldana, F.; Blanchard, M.; Kharoubi Hess, S.; Lannes, N.; Mantel, P.; Filgueira, L.; Walch, M. Silver-nanoparticles increase bactericidal activity and radical oxygen responses against bacterial pathogens in human osteoclasts. *Nanomedicine: Nanotechnology, Biology, and Medicine* **2018**, *14*, 601−607.
(38) Pauksch, L.; Rohnke, M.; Schnettler, R.; Lips, K. Silver nanoparticles do not alter human osteoclastogenesis but induce cellular uptake. *Toxicology Reports* **2014**, *1*, 900−908.
(39) Lee, C.; Lin, T.; Hwang, L.; Kuo, C.; Huang, X.; Chen, Y.; Ou, S.; Ma, C.; Chen, S.; Hsueh, Y.; Wu, C. Electrochemical synthesis of a composite coating with antibacterial ability on NiTi alloy. *Prog. Org. Coat.* **2020**, *146*, No. 105711.
(40) Ibrahim, M.; Hamzah, E.; Saud, S.; Nazim, E.; Bahador, A. Silver additions influence on biomedical porous Ti-Ni SMAS fabricated by microwave sintering. *J. Teknol.* **2018**, *80*, 97−102, DOI: 10.11113/jt.v80.11766.
(41) Goodman, S.; Yao, Z.; Keeney, M.; Yang, F. The future of biologic coatings for orthopaedic implants. *Biomaterials* **2013**, *34*, 3174−3183.
(42) Marchenko, E.; Baigonakova, G.; Larikov, V.; Monogenov, A.; Yasenchuk, Y. Structure and mechanical properties of porous TiNi alloys with Ag nanoparticles. *Coatings* **2023**, *13*, 24 DOI: 10.3390/coatings13010024.
(43) Heidenau, F.; Mittelmeier, W.; Detsch, R.; Haenle, M.; Stenzel, F.; Ziegler, G. A novel antibacterial titania coating: metal ion toxicity and in vitro surface colonization. *J. Mater. Sci. Mater. Med.* **2005**, *16*, 883−888.
(44) Tweden, K.; Cameron, J.; Razzouk, A.; Holmberg, W.; Kelly, S. Biocompatibility of silver-modified polyester for antimicrobial protection of prosthetic valves. *J. Heart Valve Dis.* **1997**, *6*, 553−561.
(45) Gosheger, G.; Hardes, J.; Ahrens, H.; Streitburger, A.; Buerger, H.; Erren, M. Silver-coated megaendoprostheses in a rabbit model − an analysis of the infection rate and toxicological side effects. *Biomaterials* **2004**, *25*, 5547−5556.
(46) Zheng, Y.; Zhang, B.; Wang, B.; Wang, Y.; Li, L.; Yang, Q.; Cui, L. Introduction of antibacterial function into biomedical TiNi shape memory alloy by the addition of element Ag. *Acta Biomater* **2011**, *7*, 2758−2767.
(47) McDonnell, G.; Russell, A. Antiseptics and disinfectants: activity, action, and resistance. *Clin. Microbiol. Rev.* **1999**, *12*, 147−179.
(48) Boudreau, M.; Imam, M.; Paredes, A.; Bryant, M.; Cunningham, C.; Felton, R.; Jones, M.; Davis, K.; Olson, G. Differential effects of silver nanoparticles and silver ions on tissue accumulation, distribution, and toxicity in the sprague dawley rat following daily oral gavage administration for 13 weeks. *Toxicol. Sci.* **2016**, *150*, 131−160.
(49) Guo, H.; Zhang, J.; Boudreau, M.; Meng, J.; Yin, J.; Liu, J.; Xu, H. Intravenous administration of silver nanoparticles causes organ toxicity through intracellular ROS-related loss of inter-endothelial junction. *Part. Fibre Toxicol.* **2016**, *13*, 21 DOI: 10.1186/s12989-016-0133-9.
(50) Trbojevich, R.; Fernandez, A.; Watanabe, F.; Mustafa, T.; Bryant, M. Comparative study of silver nanoparticle permeation using side-bi-side and Franz diffusion cells. *J. Nanopart. Res.* **2016**, *18*, 1−12.
(51) Williams, K.; Gokulan, M. K.; Cerniglia, C.; Khare, S. Size and dose dependent effects of silver nanoparticle exposure on intestinal permeability in an in vitro model of the human gut epithelium. *J. Nanobiotechnology* **2016**, *14*, 62 DOI: 10.1186/s12951-016-0214-9.
(52) Griffitt, R.; Luo, J.; Gao, J.; Bonzongo, J.; Barber, D. Effects of particle composition and species on toxicity of metallic nanomaterials in aquatic organisms. *Environ. Toxicol. Chem.* **2008**, *27*, 1972−1978.
(53) Mueller, N.; Nowack, B. Exposure modeling of engineered nanoparticles in the environment. *Environ. Sci. Technol.* **2008**, *42*, 4447−4453.

https://doi.org/10.1021/acsomega.3c08163
ACS Omega 2024, 9, 25638−25645

(54) Gunther, V.; Radkevich, A.; Kang, S.; Chekalkin, T.; Marchenko, E.; Gyunter, S. Study of the knitted TiNi mesh graft in a rabbit cranioplasty model. *Biomed. Phys. Eng. Express* **2019**, *5*, No. 027005.
(55) Topolnitskiy, E. B.; Shefer, N. A.; Marchenko, E. S.; Mikhed, R. A. Thoracoscopic repair of posttraumatic phrenic hernia in 62 years after injury of the diaphragm. *Khirurgiia (Mosk)* **2022**, No. 2, 62−66.
(56) Lemaire, V.; Tobin, F.; Greller, L.; Cho, C.; Suva, L. Modeling the interactions between osteoblast and osteoclast activities in bone remodeling. *J. Theor. Biol.* **2004**, *229*, 293−309.
(57) Zhu, Y.; Zhou, D.; Zan, X.; Sheng, S.; Ye, Q. Engineering the surfaces of orthopaedic implants with osteogenesis and antioxidants to enhance bone formation in vitro and in vivo. *Colloids Surf., B* **2022**, *212*, No. 112319.
(58) Chandra, G.; Pandey, A. Biodegradable bone implants in orthopedic applications: a review. *Biocybern. Biomed. Eng.* **2020**, *40* (2), 596−610.
(59) Zheng, Y.; Zhang, B.; Wang, B.; Wang, Y.; Li, L.; Yang, Q.; Cui, L. Introduction of antibacterial function into biomedical TiNi shape memory alloy by the addition of element Ag. *Acta Biomater.* **2011**, *7*, 2758−2767.
(60) Oh, K.; Joo, U.; Park, G.; Hwang, C.; Kim, K. Effect of silver addition on the properties of nickel-titanium alloys for dental application. *J. Biomed. Mater. Res. B: Appl. Biomater.* **2006**, *76*, 306−314.
(61) Marchenko, E.; Baigonakova, G.; Kokorev, O.; Klopotov, A. A.; Iuzhakov, M. Phase equilibrium, structure, mechanical and biocompatible properties of TiNi-based alloy with silver. *Mater. Res. Express* **2019**, *6*, No. 066559.
(62) Otsuka, K.; Ren, X. Physical metallurgy of Ti-Ni-based shape memory alloys. *Prog. Mater. Sci.* **2005**, *50*, 511−678.
(63) Marchenko, E.; Yasenchuk, Y.; Baigonakova, G.; Gunther, S.; Yuzhakov, M.; Zenkin, S.; Potekaev, A.; Dubovikov, K. Phase formation during air annealing of Ti−Ni−Ti laminate. *Surf. Coat. Technol.* **2020**, *388*, No. 125543.

https://doi.org/10.1021/acsomega.3c08163
ACS Omega 2024, 9, 25638−25645